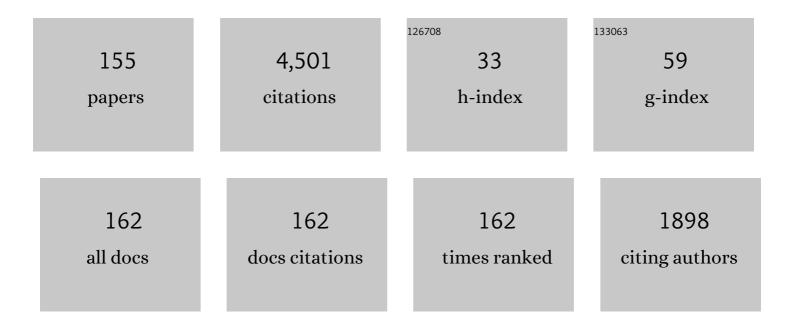
M-C Fok

List of Publications by Year in descending order

Source: https://exaly.com/author-pdf/2155516/publications.pdf Version: 2024-02-01



M-C FOR

#	Article	IF	CITATIONS
1	Soft Xâ€ray and ENA Imaging of the Earth's Dayside Magnetosphere. Journal of Geophysical Research: Space Physics, 2021, 126, e2020JA028816.	0.8	13
2	Magnetotailâ€Inner Magnetosphere Transport Associated With Fast Flows Based on Combined Globalâ€Hybrid and CIMI Simulation. Journal of Geophysical Research: Space Physics, 2021, 126, e2020JA028405.	0.8	6
3	Observations of Density Cavities and Associated Warm Ion Flux Enhancements in the Inner Magnetosphere. Journal of Geophysical Research: Space Physics, 2021, 126, e2020JA028326.	0.8	3
4	New Developments in the Comprehensive Inner Magnetosphereâ€Ionosphere Model. Journal of Geophysical Research: Space Physics, 2021, 126, e2020JA028987.	0.8	8
5	Comparison of CIMI Simulations and TWINS Observations on June 28 and 29, 2013. Journal of Geophysical Research: Space Physics, 2021, 126, e2020JA028388.	0.8	0
6	Relative Contribution of ULF Waves and Whistlerâ€mode Chorus to the Radiation Belt Variation during the May 2017 Storm. Journal of Geophysical Research: Space Physics, 2021, 126, e2020JA028972.	0.8	1
7	A Case Study on the Origin of Nearâ€Earth Plasma. Journal of Geophysical Research: Space Physics, 2020, 125, e2020JA028205.	0.8	23
8	Does Ring Current Heating Generate the Observed O ⁺ Shell?. Geophysical Research Letters, 2020, 47, e2020GL088419.	1.5	3
9	Local Heating of Oxygen Ions in the Presence of Magnetosonic Waves: Possible Source for the Warm Plasma Cloak?. Journal of Geophysical Research: Space Physics, 2020, 125, e2019JA027210.	0.8	12
10	Cross-regional coupling. , 2020, , 225-244.		3
11	Nonlinear Wave Growth Analysis of Whistlerâ€Mode Chorus Generation Regions Based on Coupled MHD and Advection Simulation of the Inner Magnetosphere. Journal of Geophysical Research: Space Physics, 2020, 125, e2019JA026951.	0.8	3
12	Contribution of ULF Wave Activity to the Global Recovery of the Outer Radiation Belt During the Passage of a High‧peed Solar Wind Stream Observed in September 2014. Journal of Geophysical Research: Space Physics, 2019, 124, 1660-1678.	0.8	14
13	On the Contribution of EMIC Waves to the Reconfiguration of the Relativistic Electron Butterfly Pitch Angle Distribution Shape on 2014 September 12—A Case Study*. Astrophysical Journal, 2019, 872, 36.	1.6	8
14	Initial Results From the GEM Challenge on the Spacecraft Surface Charging Environment. Space Weather, 2019, 17, 299-312.	1.3	17
15	Wave-induced particle precipitation into the ionosphere from the inner magnetosphere. , 2019, , .		0
16	Geomagnetic Storms: First-Principles Models for Extreme Geospace Environment. , 2018, , 231-258.		3
17	The Unknown Hydrogen Exosphere: Space Weather Implications. Space Weather, 2018, 16, 205-215.	1.3	20
18	An Energetic Electron Flux Dropout Due to Magnetopause Shadowing on 1 June 2013. Journal of Geophysical Research: Space Physics, 2018, 123, 1178-1190.	0.8	16

#	Article	IF	CITATIONS
19	Dynamics of a geomagnetic storm on 7–10 September 2015 as observed by TWINS and simulated by CIMI. Annales Geophysicae, 2018, 36, 1439-1456.	0.6	4
20	Including Kinetic Ion Effects in the Coupled Global Ionospheric Outflow Solution. Journal of Geophysical Research: Space Physics, 2018, 123, 2851-2871.	0.8	21
21	Imaging Plasma Density Structures in the Soft X-Rays Generated by Solar Wind Charge Exchange with Neutrals. Space Science Reviews, 2018, 214, 1.	3.7	47
22	Global Distribution of ULF Waves During Magnetic Storms: Comparison of Arase, Ground Observations, and BATSRUSÂ+ÂCRCM Simulation. Geophysical Research Letters, 2018, 45, 9390-9397.	1.5	7
23	Magnetosphere dynamics during the 14ÂNovember 2012 storm inferred from TWINS, AMPERE, Van Allen Probes, and BATS-R-US–CRCM. Annales Geophysicae, 2018, 36, 107-124.	0.6	8
24	Theory, modeling, and integrated studies in the Arase (ERG) project. Earth, Planets and Space, 2018, 70, .	0.9	11
25	A new solar windâ€driven global dynamic plasmapause model: 2. Model and validation. Journal of Geophysical Research: Space Physics, 2017, 122, 7172-7187.	0.8	24
26	A scheme for forecasting severe space weather. Journal of Geophysical Research: Space Physics, 2017, 122, 2824-2835.	0.8	28
27	CIMI simulations with newly developed multiparameter chorus and plasmaspheric hiss wave models. Journal of Geophysical Research: Space Physics, 2017, 122, 9344-9357.	0.8	17
28	A new solar windâ€driven global dynamic plasmapause model: 1. Database and statistics. Journal of Geophysical Research: Space Physics, 2017, 122, 7153-7171.	0.8	16
29	Impact of substorm time O ⁺ outflow on ring current enhancement. Journal of Geophysical Research: Space Physics, 2017, 122, 6304-6317.	0.8	8
30	Electron Drift Resonance in the MHD oupled Comprehensive Inner Magnetosphereâ€ l onosphere Model. Journal of Geophysical Research: Space Physics, 2017, 122, 12,006.	0.8	12
31	Simulation of a rapid dropout event for highly relativistic electrons with the RBE model. Journal of Geophysical Research: Space Physics, 2016, 121, 4092-4102.	0.8	19
32	Special issue "The 12th International Conference on Substorms― Earth, Planets and Space, 2016, 68, .	0.9	0
33	Global images of trapped ring current ions during main phase of 17 March 2015 geomagnetic storm as observed by TWINS. Journal of Geophysical Research: Space Physics, 2016, 121, 6509-6525.	0.8	18
34	Convective growth of electromagnetic ion cyclotron waves from realistic ring current ion distributions. Journal of Geophysical Research: Space Physics, 2016, 121, 10,966.	0.8	14
35	Inverse energy dispersion of energetic ions observed in the magnetosheath. Geophysical Research Letters, 2016, 43, 7338-7347.	1.5	5
36	Determination of the Earth's plasmapause location from the CEâ€3 EUVC images. Journal of Geophysical Research: Space Physics, 2016, 121, 296-304.	0.8	18

#	Article	IF	CITATIONS
37	Estimation of pitch angle diffusion rates and precipitation time scales of electrons due to EMIC waves in a realistic field model. Journal of Geophysical Research: Space Physics, 2015, 120, 8529-8546.	0.8	17
38	TWINS stereoscopic imaging of multiple peaks in the ring current. Journal of Geophysical Research: Space Physics, 2015, 120, 368-383.	0.8	22
39	Comprehensive analysis of the flux dropout during 7–8 November 2008 storm using multisatellite observations and RBE model. Journal of Geophysical Research: Space Physics, 2015, 120, 4298-4312.	0.8	5
40	Magnetospheric boundary perturbations on MHD and kinetic scales. Journal of Geophysical Research: Space Physics, 2015, 120, 113-137.	0.8	6
41	Large magnetic storms as viewed by TWINS: A study of the differences in the medium energy ENA composition. Journal of Geophysical Research: Space Physics, 2014, 119, 2819-2835.	0.8	19
42	The Comprehensive Inner Magnetosphereâ€ŀonosphere Model. Journal of Geophysical Research: Space Physics, 2014, 119, 7522-7540.	0.8	106
43	Solar filament impact on 21 January 2005: Geospace consequences. Journal of Geophysical Research: Space Physics, 2014, 119, 5401-5448.	0.8	20
44	The ionospheric outflow feedback loop. Journal of Atmospheric and Solar-Terrestrial Physics, 2014, 115-116, 59-66.	0.6	24
45	Estimation of temporal evolution of the helium plasmasphere based on a sequence of IMAGE/EUV images. Journal of Geophysical Research: Space Physics, 2014, 119, 3708-3723.	0.8	8
46	Estimation of the helium ion density distribution in the plasmasphere based on a single IMAGE/EUV image. Journal of Geophysical Research: Space Physics, 2014, 119, 3724-3740.	0.8	6
47	Superposed epoch analyses of ion temperatures during CME- and CIR/HSS-driven storms. Journal of Atmospheric and Solar-Terrestrial Physics, 2014, 115-116, 67-78.	0.6	18
48	Pressure anisotropy in global magnetospheric simulations: Coupling with ring current models. Journal of Geophysical Research: Space Physics, 2013, 118, 5639-5658.	0.8	24
49	Non-linear whistler mode wave effects on magnetospheric energetic electrons. Journal of Atmospheric and Solar-Terrestrial Physics, 2013, 102, 8-16.	0.6	4
50	Effects of different geomagnetic storm drivers on the ring current: CRCM results. Journal of Geophysical Research: Space Physics, 2013, 118, 1062-1073.	0.8	28
51	Simulated ring current response during periods of dawn-dusk oriented interplanetary magnetic field (By). Journal of Geophysical Research: Space Physics, 2013, 118, 2228-2243.	0.8	2
52	CRCM + BATS‒R‒US two‒way coupling. Journal of Geophysical Research: Space Physics, 2013, 118, 1635-	16508	72
53	Comparative analysis of low-altitude ENA emissions in two substorms. Journal of Geophysical Research: Space Physics, 2013, 118, 724-731.	0.8	20
54	Oxygenâ€hydrogen differentiated observations from TWINS: The 22 July 2009 storm. Journal of Geophysical Research: Space Physics, 2013, 118, 3377-3393.	0.8	21

#	Article	IF	CITATIONS
55	Moonâ€based EUV imaging of the Earth's Plasmasphere: Model simulations. Journal of Geophysical Research: Space Physics, 2013, 118, 7085-7103.	0.8	25
56	Inversion of the Earth's Plasmaspheric Density Distribution from EUV Images with Genetic Algorithm. Chinese Journal of Geophysics, 2012, 55, 1-9.	0.2	13
5 7	Plasmaspheric trough evolution under different conditions of subauroral ion drift. Science China Technological Sciences, 2012, 55, 1287-1294.	2.0	12
58	Electron energy diffusion and advection due to non-linear electron-chorus wave interactions. Journal of Atmospheric and Solar-Terrestrial Physics, 2012, 80, 152-160.	0.6	12
59	Remote observations of ion temperatures in the quiet time magnetosphere. Geophysical Research Letters, 2011, 38, n/a-n/a.	1.5	26
60	Modeling the superstorm in November 2003. Journal of Geophysical Research, 2011, 116, n/a-n/a.	3.3	18
61	Rapid decay of storm time ring current due to pitch angle scattering in curved field line. Journal of Geophysical Research, 2011, 116, .	3.3	32
62	Reconstruction of the plasmasphere from Moon-based EUV images. Journal of Geophysical Research, 2011, 116, n/a-n/a.	3.3	11
63	Rapid rebuilding of the outer radiation belt. Journal of Geophysical Research, 2011, 116, n/a-n/a.	3.3	31
64	Recent developments in the radiation belt environment model. Journal of Atmospheric and Solar-Terrestrial Physics, 2011, 73, 1435-1443.	0.6	63
65	Effects of energy and pitch angle mixed diffusion on radiation belt electrons. Journal of Atmospheric and Solar-Terrestrial Physics, 2011, 73, 785-795.	0.6	10
66	On the effect of IMF turning on ion dynamics at Mercury. Annales Geophysicae, 2011, 29, 987-996.	0.6	4
67	Calculation of the extreme ultraviolet radiation of the earth's plasmasphere. Science China Technological Sciences, 2010, 53, 200-205.	2.0	9
68	lon dynamics during compression of Mercury's magnetosphere. Annales Geophysicae, 2010, 28, 1467-1474.	0.6	10
69	Dynamics of ring current and electric fields in the inner magnetosphere during disturbed periods: CRCM–BATSâ€Râ€US coupled model. Journal of Geophysical Research, 2010, 115, .	3.3	42
70	Effects of plasma sheet properties on stormâ€ŧime ring current. Journal of Geophysical Research, 2010, 115, .	3.3	6
71	Ring current dynamics in moderate and strong storms: Comparative analysis of TWINS and IMAGE/HENA data with the Comprehensive Ring Current Model. Journal of Geophysical Research, 2010, 115, .	3.3	39
72	Evolution of lowâ€altitude and ring current ENA emissions from a moderate magnetospheric storm: Continuous and simultaneous TWINS observations. Journal of Geophysical Research, 2010, 115, .	3.3	39

#	Article	IF	CITATIONS
73	Simulation and TWINS observations of the 22 July 2009 storm. Journal of Geophysical Research, 2010, 115, .	3.3	26
74	Global response to local ionospheric mass ejection. Journal of Geophysical Research, 2010, 115, .	3.3	7
75	Integration of the radiation belt environment model into the space weather modeling framework. Journal of Atmospheric and Solar-Terrestrial Physics, 2009, 71, 1653-1663.	0.6	29
76	Selfâ€consistent model of magnetospheric electric field, ring current, plasmasphere, and electromagnetic ion cyclotron waves: Initial results. Journal of Geophysical Research, 2009, 114, .	3.3	23
77	Dynamical property of storm time subauroral rapid flows as a manifestation of complex structures of the plasma pressure in the inner magnetosphere. Journal of Geophysical Research, 2009, 114, .	3.3	31
78	Controlling factors of Region 2 field-aligned current and its relationship to the ring current: Model results. Advances in Space Research, 2008, 41, 1234-1242.	1.2	3
79	A method for estimating the ring current structure and the electric potential distribution using energetic neutral atom data assimilation. Journal of Geophysical Research, 2008, 113, .	3.3	17
80	On ionospheric trough conductance and subauroral polarization streams: Simulation results. Journal of Geophysical Research, 2008, 113, .	3.3	41
81	Radiation Belt Environment model: Application to space weather nowcasting. Journal of Geophysical Research, 2008, 113, .	3.3	140
82	Twoâ€dimensional observations of overshielding during a magnetic storm by the Super Dual Auroral Radar Network (SuperDARN) Hokkaido radar. Journal of Geophysical Research, 2008, 113, .	3.3	41
83	A comparison of Neutral Atom Detector Unit neutral atom image inversion with a comprehensive ring current model. Journal of Geophysical Research, 2008, 113, .	3.3	3
84	Role of periodic loadingâ€unloading in the magnetotail versus interplanetary magnetic field <i>B</i> _{<i>z</i>} flipping in the ring current buildup. Journal of Geophysical Research, 2008, 113, .	3.3	1
85	Generation of plasmaspheric undulations. Geophysical Research Letters, 2008, 35, .	1.5	9
86	Plasma plume circulation and impact in an MHD substorm. Journal of Geophysical Research, 2008, 113, .	3.3	23
87	Viewing perspective in energetic neutral atom intensity. Journal of Geophysical Research, 2008, 113, .	3.3	6
88	Magnetic coupling of the ring current and the radiation belt. Journal of Geophysical Research, 2008, 113, .	3.3	34
89	Tailward flow of energetic neutral atoms observed at Venus. Journal of Geophysical Research, 2008, 113, .	3.3	20
90	Tailward flow of energetic neutral atoms observed at Mars. Journal of Geophysical Research, 2008, 113, .	3.3	30

#	Article	IF	CITATIONS
91	Buildup of the ring current during periodic loadingâ€unloading cycles in the magnetotail driven by steady southward interplanetary magnetic field. Journal of Geophysical Research, 2007, 112, .	3.3	12
92	Ion energization during substorms at Mercury. Planetary and Space Science, 2007, 55, 1502-1508.	0.9	16
93	Global aspects of solar wind–ionosphere interactions. Journal of Atmospheric and Solar-Terrestrial Physics, 2007, 69, 265-278.	0.6	25
94	Proton auroral intensifications and injections at synchronous altitude. Geophysical Research Letters, 2006, 33, .	1.5	3
95	Relationship between Region 2 field-aligned current and the ring current: Model results. Journal of Geophysical Research, 2006, 111, .	3.3	24
96	Modeling global O+ substorm injection using analytic magnetic field model. Journal of Geophysical Research, 2006, 111, .	3.3	20
97	X-ray emission from the terrestrial magnetosheath including the cusps. Journal of Geophysical Research, 2006, 111, .	3.3	50
98	Characteristics of 2–6 MeV electrons in the slot region and inner radiation belt. Journal of Geophysical Research, 2006, 111, .	3.3	31
99	Impulsive enhancements of oxygen ions during substorms. Journal of Geophysical Research, 2006, 111, .	3.3	99
100	Correction to "Ring current and the magnetosphere-ionosphere coupling during the superstorm of 20 November 2003― Journal of Geophysical Research, 2005, 110, .	3.3	1
101	Solar and ionospheric plasmas in the ring current region. Geophysical Monograph Series, 2005, , 179-194.	0.1	12
102	Energetic particle injections into the outer cusp during compression events. Earth, Planets and Space, 2005, 57, 125-130.	0.9	4
103	Ring current and the magnetosphere-ionosphere coupling during the superstorm of 20 November 2003. Journal of Geophysical Research, 2005, 110, .	3.3	78
104	Nonlinear impact of plasma sheet density on the storm-time ring current. Journal of Geophysical Research, 2005, 110, .	3.3	34
105	Plasma sheet and (nonstorm) ring current formation from solar and polar wind sources. Journal of Geophysical Research, 2005, 110, .	3.3	43
106	Low-energy neutral atom signatures of magnetopause motion in response to southwardBz. Journal of Geophysical Research, 2005, 110, .	3.3	28
107	Effect of multiple substorms on the buildup of the ring current. Journal of Geophysical Research, 2005, 110, .	3.3	9
108	Magnetosheath variations during the storm main phase on 20 November 2003: Evidence for solar wind density control of energy transfer to the magnetosphere. Geophysical Research Letters, 2005, 32, .	1.5	20

#	Article	IF	CITATIONS
109	Monitoring the high-altitude cusp with the Low Energy Neutral Atom imager: Simultaneous observations from IMAGE and Polar. Journal of Geophysical Research, 2005, 110, .	3.3	12
110	Geospace storm processes coupling the ring current, radiation belt and plasmasphere. Geophysical Monograph Series, 2005, , 207-220.	0.1	15
111	Magnetospheric convection electric field dynamics andstormtime particle energization: case study of the magneticstorm of 4 May 1998. Annales Geophysicae, 2004, 22, 497-510.	0.6	34
112	Neutral atom imaging of solar wind interaction with the Earth and Venus. Journal of Geophysical Research, 2004, 109, .	3.3	16
113	Response of neutral atom emissions in the low-latitude and high-latitude magnetosheath direction to the magnetopause motion under extreme solar wind conditions. Journal of Geophysical Research, 2004, 109, .	3.3	16
114	Stormtime particle energization with high temporal resolution AMIE potentials. Journal of Geophysical Research, 2004, 109, .	3.3	23
115	Influence of ionosphere conductivity on the ring current. Journal of Geophysical Research, 2004, 109,	3.3	49
116	Postmidnight storm-time enhancement of tens-of-keV proton flux. Journal of Geophysical Research, 2004, 109, .	3.3	57
117	Global ena Image Simulations. Space Science Reviews, 2003, 109, 77-103.	3.7	107
118	Heliosphere-Geosphere Interactions Using Low Energy Neutral Atom Imaging. Space Science Reviews, 2003, 109, 351-371.	3.7	17
119	Self-consistent magnetosphere-ionosphere coupling: Theoretical studies. Journal of Geophysical Research, 2003, 108, .	3.3	38
120	Correction to "Self-Consistent Magnetosphere-Ionosphere Coupling: Theoretical Studies― Journal of Geophysical Research, 2003, 108, .	3.3	1
121	A radiation belt-ring current forecasting model. Space Weather, 2003, 1, n/a-n/a.	1.3	26
122	Global ENA IMAGE Simulations. , 2003, , 77-103.		7
123	Global ENA observations of the storm mainphase ring current: Implications for skewed electric fields in the inner magnetosphere. Geophysical Research Letters, 2002, 29, 15-1-15-3.	1.5	92
124	The dayside reconnection X line. Journal of Geophysical Research, 2002, 107, SMP 26-1.	3.3	92
125	Rapid enhancement of radiation belt electron fluxes due to substorm dipolarization of the geomagnetic field. Journal of Geophysical Research, 2001, 106, 3873-3881.	3.3	64
126	Comprehensive computational model of Earth's ring current. Journal of Geophysical Research, 2001, 106, 8417-8424.	3.3	246

#	Article	IF	CITATIONS
127	Observations of neutral atoms from the solar wind. Journal of Geophysical Research, 2001, 106, 24893-24906.	3.3	56
128	Ring Currents and Internal Plasma Sources. Space Science Reviews, 2001, 95, 555-568.	3.7	29
129	The plasma sheet source groove. Journal of Atmospheric and Solar-Terrestrial Physics, 2000, 62, 505-512.	0.6	8
130	lmaging a geomagnetic storm with energetic neutral atoms. Journal of Atmospheric and Solar-Terrestrial Physics, 2000, 62, 911-917.	0.6	3
131	Medium energy neutral atom (MENA) imager for the IMACE mission. Space Science Reviews, 2000, 91, 113-154.	3.7	90
132	Deconvolution of Energetic Neutral Atom Images of the Earth's Magnetosphere. Space Science Reviews, 2000, 91, 421-436.	3.7	32
133	Quantitative modeling of modulated ion injections observed by Polar-Thermal Ion Dynamics Experiment in the cusp region. Journal of Geophysical Research, 2000, 105, 25191-25203.	3.3	7
134	On the relative importance of convection and temperature to the behavior of the ionosphere in North America during January 6-12, 1997. Journal of Geophysical Research, 2000, 105, 12763-12776.	3.3	49
135	Medium Energy Neutral Atom (MENA) Imager for the Image Mission. , 2000, , 113-154.		16
136	Deconvolution of Energetic Neutral Atom Images of the Earth's Magnetosphere. , 2000, , 421-436.		3
137	Modeling of inner plasma sheet and ring current during substorms. Journal of Geophysical Research, 1999, 104, 14557-14569.	3.3	112
138	The role of precipitation losses in producing the rapid early recovery phase of the Great Magnetic Storm of February 1986. Journal of Geophysical Research, 1998, 103, 6801-6814.	3.3	84
139	Ring current modeling in a realistic magnetic field configuration. Geophysical Research Letters, 1997, 24, 1775-1778.	1.5	82
140	Global, collisional model of high-energy photoelectrons. Geophysical Research Letters, 1996, 23, 331-334.	1.5	21
141	Ring current development during storm main phase. Journal of Geophysical Research, 1996, 101, 15311-15322.	3.3	158
142	Plasmasphere modeling with ring current heating. Geophysical Monograph Series, 1995, , 173-175.	0.1	0
143	Ring current-plasmasphere coupling through Coulomb collisions. Geophysical Monograph Series, 1995, , 161-171.	0.1	14
144	Microscale effects from global hot plasma imagery. Geophysical Monograph Series, 1995, , 37-46.	0.1	7

#	Article	IF	CITATIONS
145	Three-Dimensional Ring Current Decay Model. Journal of Geophysical Research, 1995, 100, 9619.	3.3	145
146	A bounce-averaged kinetic model of the ring current ion population. Geophysical Research Letters, 1994, 21, 2785-2788.	1.5	77
147	Decay of equatorial ring current ions and associated aeronomical consequences. Journal of Geophysical Research, 1993, 98, 19381-19393.	3.3	151
148	Solar cycle variation in the subauroral electron temperature enhancement: Comparison of AE and DE 2 satellite observations. Journal of Geophysical Research, 1991, 96, 1861-1866.	3.3	16
149	Lifetime of ring current particles due to coulomb collisions in the plasmasphere. Journal of Geophysical Research, 1991, 96, 7861-7867.	3.3	143
150	Seasonal variations in the subauroral electron temperature enhancement. Journal of Geophysical Research, 1991, 96, 9773-9780.	3.3	15
151	Investigation of 3D Energetic Particle Transport Inside Quiet-Time Magnetosphere using Particle Tracing in Global MHD Model. Geophysical Monograph Series, 0, , 307-318.	0.1	3
152	Time Scales for Localized Radiation Belt Injections to Become a Thin Shell. Geophysical Monograph Series, 0, , 161-176.	0.1	2
153	Ring Current Asymmetry and the Love-Gannon Relation. Geophysical Monograph Series, 0, , 315-320.	0.1	Ο
154	Drift-Shell Splitting in an Asymmetric Magnetic Field. Geophysical Monograph Series, 0, , 327-331.	0.1	6
155	Impact of Solar Wind on the Earth Magnetosphere: Recent Progress in the Modeling of Ring Current and Radiation Belts. , 0, , .		0